PONTIFICIA UNIVERSIDAD CATÓLICA DE CHILE

Biomedical Imaging Center

iibm Instituto de Ingeniería Biológica y Médica

Imágenes Biomédicas

Pablo Irarrázaval
pim@uc.cl

¿Cuál es mi motivación?

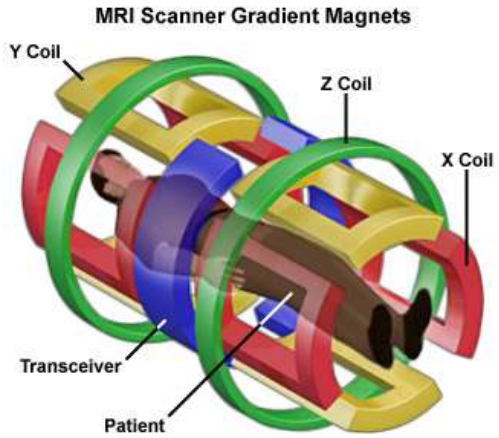

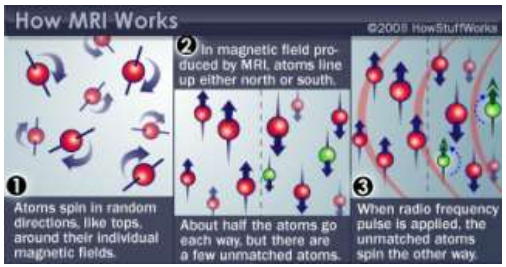

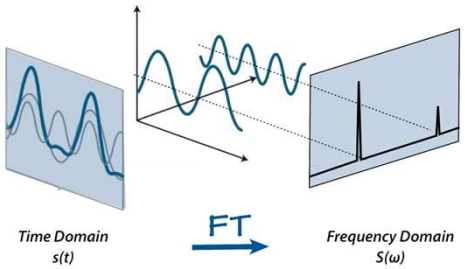

$$f(t) = \frac{1}{\sqrt{2\pi}} \int_0^{\infty} F(\omega)\, \mathrm{e}^{i\omega t}\, dt$$

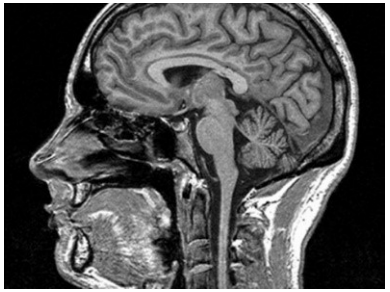

¿Cuál es mi motivación?

Mejor aún: aprendemos y lo pasamos bien

¿Cuál es mi motivación?

Mejor aún: aprendemos y lo pasamos bien

Sin dejar de ser normales!

Análisis de palabras de mis papers

iibm
Instituto de Ingeniería Biológica y Médica

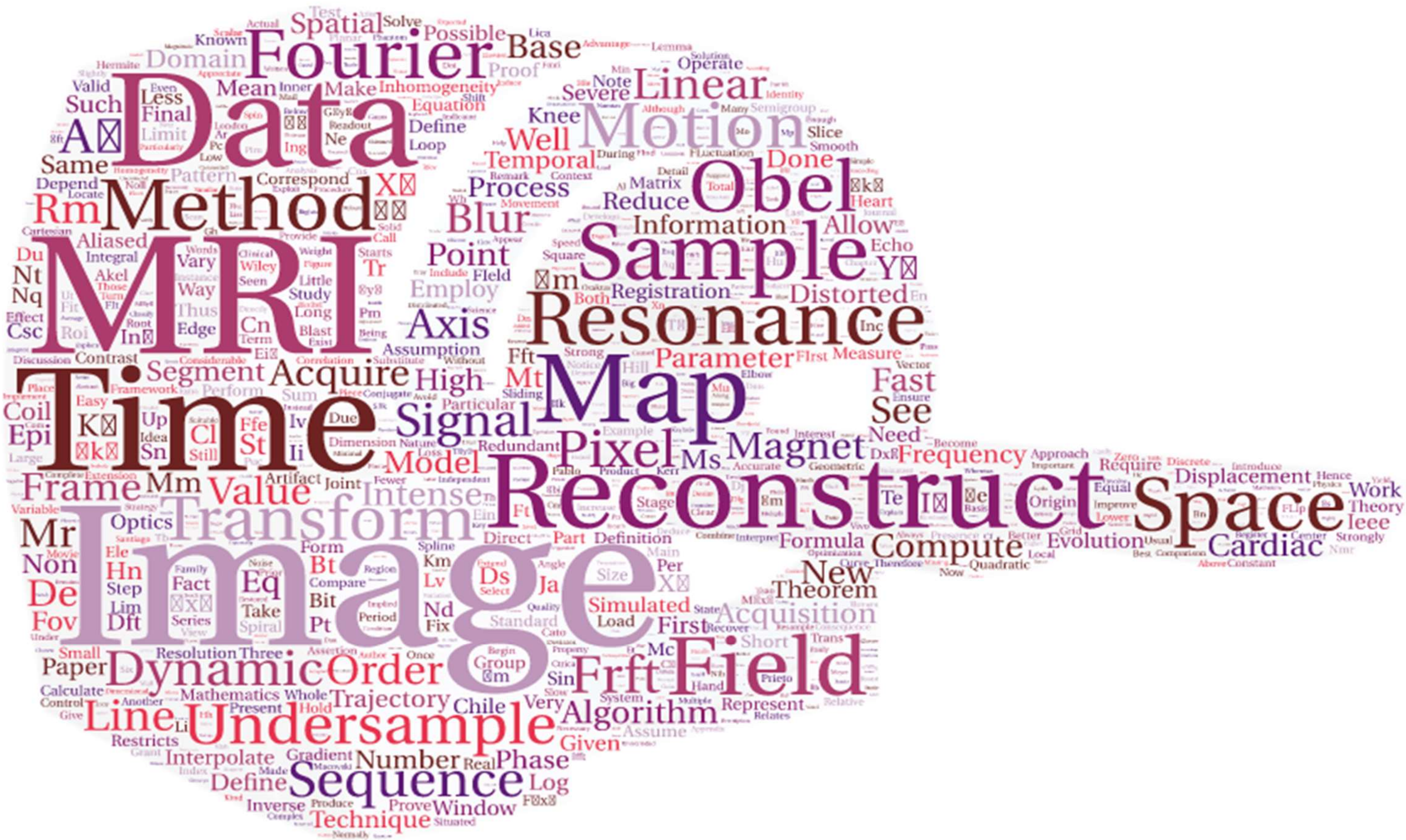

CIB: Fundado en 2000

Equipamiento con tiempo exclusivo de investigación:

- Philips Achieva 1.5 T
- Philips Ingenia 3.0 T
- Bruker Animales 1.0T
- Siemens Free.Max 0.55T

Acceso a otro equipamiento de la Red de Salud

Profesores: 12
Estudiantes: 90 (PhD, MSc)
Postdocs: 10
(Inglaterra, France, USA, Colombia, España, Chile)
Estudiantes de intercambio: 8
(Alemania, Inglaterra, España, Colombia, Japón)

Proyectos en los que participo

- FONDECYT 2021
  - “Intensity Learning for Off-Resonance Correction in MRI”
- ANILLO 2020
  - “Development of novel imaging techniques to study the brain in severe mental health disorders”
- NUCLEO MILENIO 2019-
  - “Cardiovascular MRI”
- INSTITUTO MILENIO 2022
  - “Intelligent Healthcare Engineering (iHEALTH)”
- FONDEQUIP MAYOR 2022
  - “Enabling Technology for Cutting-edge MRI Research in Chile: Towards Intelligent & Affordable Medical Imaging”

Off-resonance correction

$$s(t) = \int m(\mathbf{x}) e^{-i2\pi \mathbf{x}\cdot\mathbf{k}(t)}\, d\mathbf{x}$$

$$s(t) = \int m(\mathbf{x}) e^{-i2\pi (\mathbf{x}\cdot\mathbf{k}(t) + t\Delta f(\mathbf{x}))}\, d\mathbf{x} = \int \left\{ m(\mathbf{x}) e^{-i2\pi t \Delta f(\mathbf{x})} \right\} e^{-i2\pi \mathbf{x}\cdot\mathbf{k}(t)}\, d\mathbf{x}$$

Problema: encontrar m(x) a partir de s(t)

Sub-proyectos: SPIO

Figure 1: *SPIO nanoparticles used to detect cancer in Sentinel Lymph Nodes and Off-Resonance distortion in the breast image: place of injection (yellow arrow) and residual particles (white arrows) [24].*

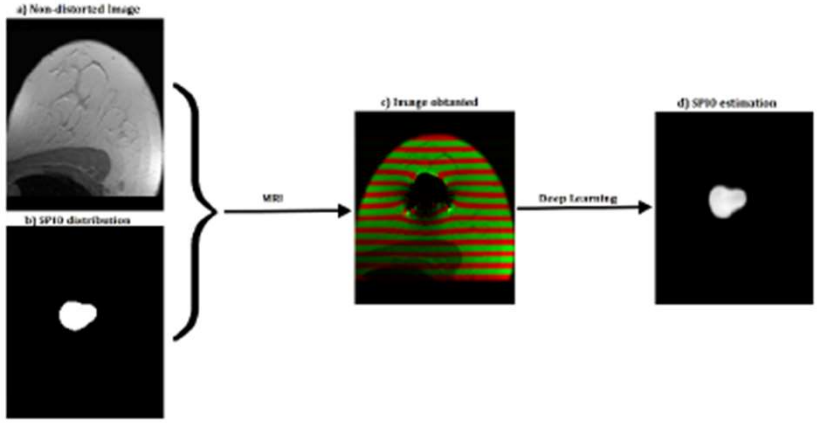

Figure 2: *View Line sequence acquisition with a simulated SPIO distribution and the reconstructed concentration using a U-Net trained with simulated data [25].*

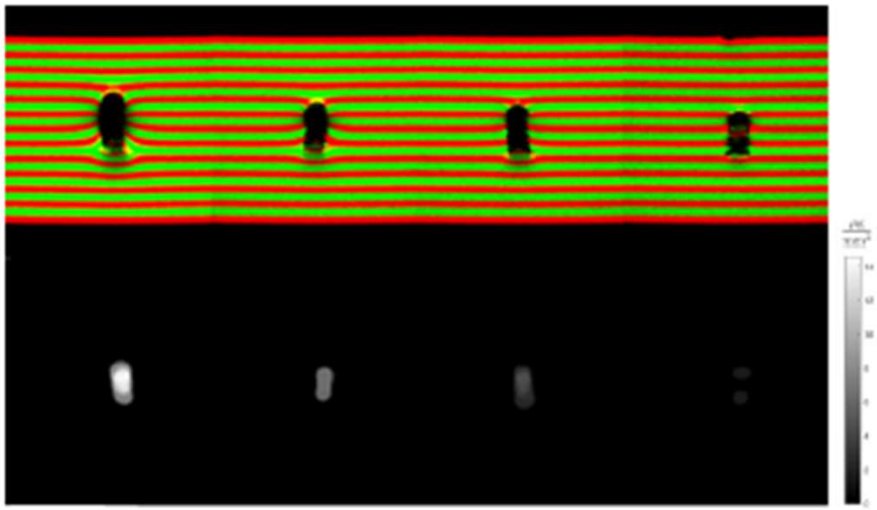

Figure 3: *Concentrations (bottom) estimated from View Line images (top) from a real sample of SPIO (Resovist) in an agar bottle, acquired in a 7T scanner.*

Spin-level simulator

Julia – Standard formats (PulseSeq, ISMRMD, DICOM) – web based

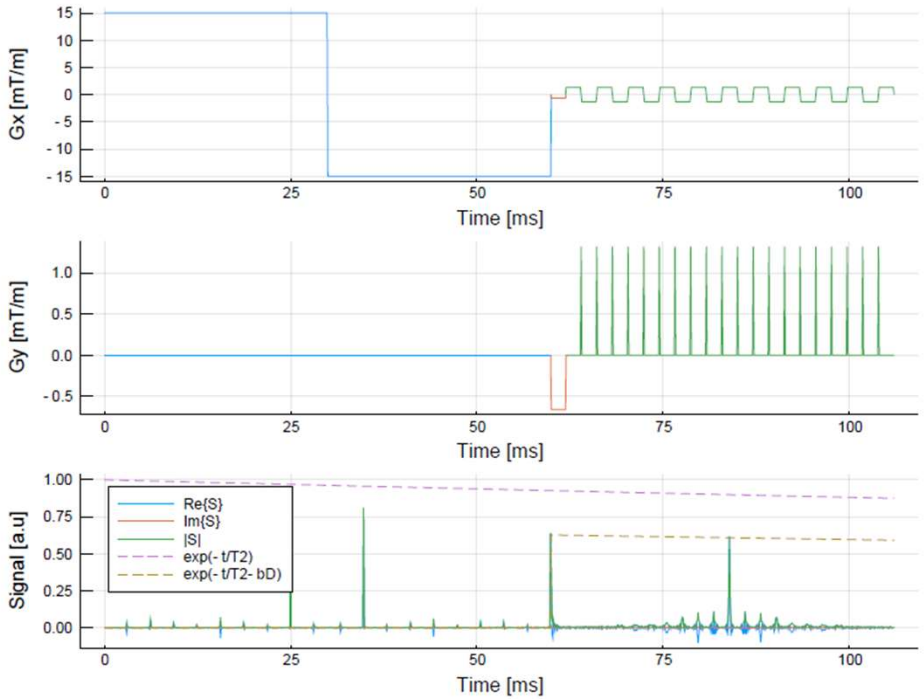

Figure 1: Example of simulated sequence, different blocks in the sequence are colored differently. In the top two rows we have the gradients and in the bottom the resulting signal, compared with the mean T2 decay and diffusion encoding.

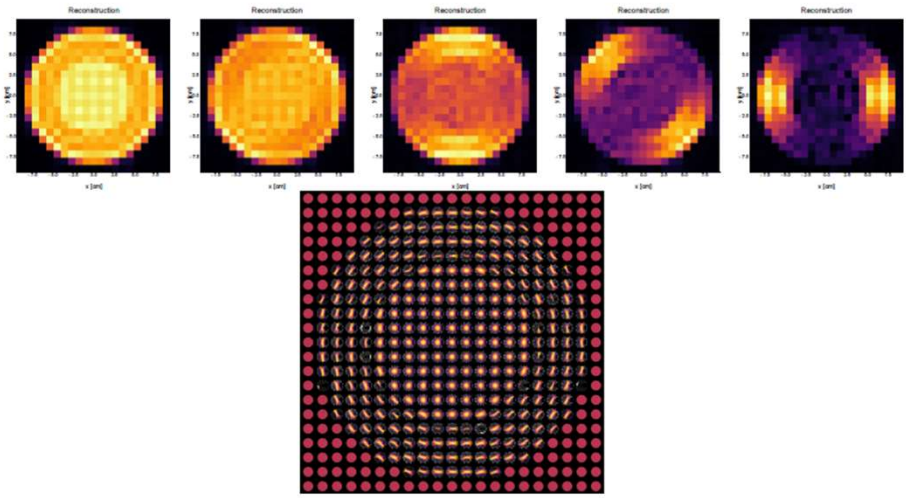

Figure 2: (Top.) Multiple DWIs generated for the static phantom showing the effect of the diffusion encoding, changing the angle of the diffusion enconding gradient and its strength. (Bottom.) Reconstructed diffusion propagators per voxel. In the center we have free diffusion and in the edges propagators in the direction of the fibers.

Desafío nuevo equipo

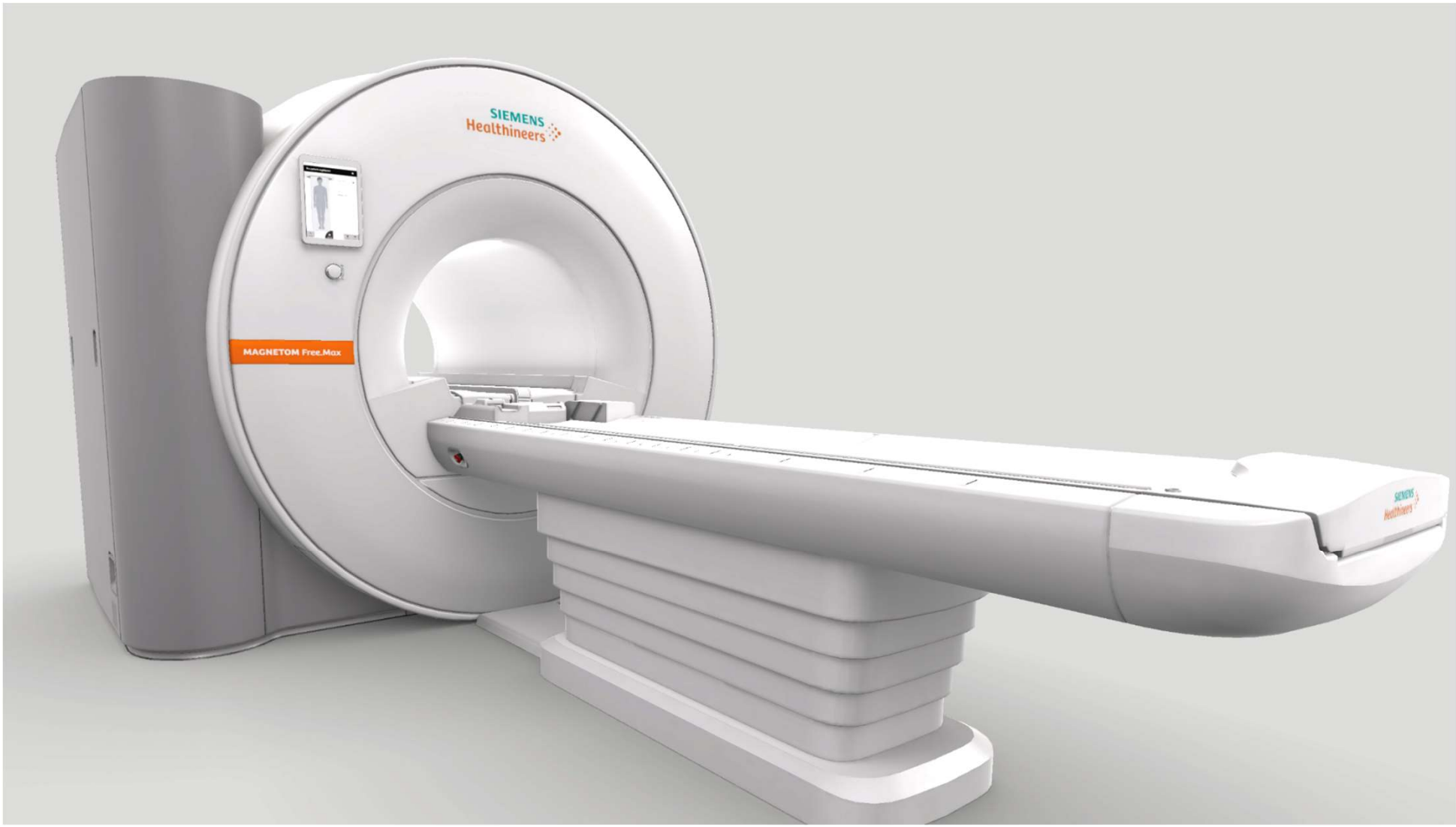

Desafío nuevo equipo

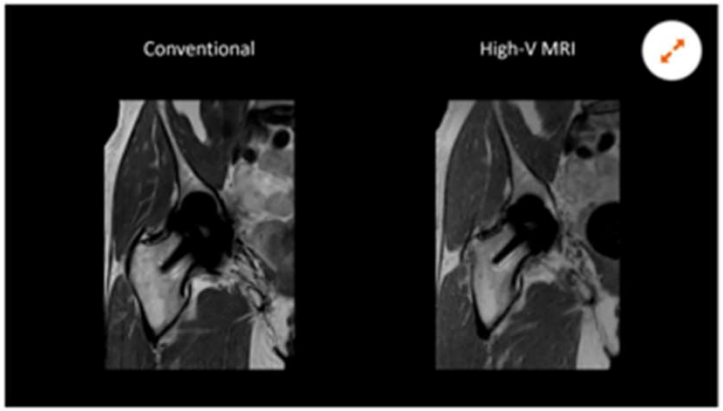

Improved implant imaging with High-V MRI

Imaging metal implants has historically been difficult with conventional MRI systems as metal causes artifacts. High-V MRI offers intrinsic physical advantages that result in reduced metal distortions and therewith strongly improved diagnostic capabilities for implant imaging.

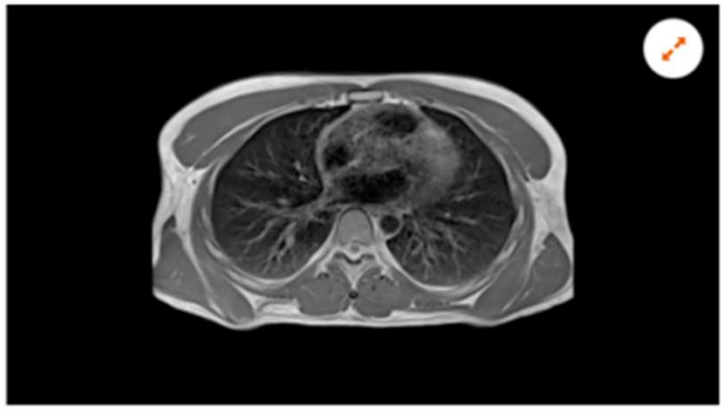

New opportunities in pulmonary imaging with High-V MRI

Pulmonary imaging has been notoriously difficult with conventional MRI as the air-tissue interfaces result in a fast signal decay. These challenges scale with magnetic field strength which makes High-V MRI the perfect opportunity for pulmonary imaging. As a result, High-V MRI provides possibilities to expand the reach of pulmonary MRI.

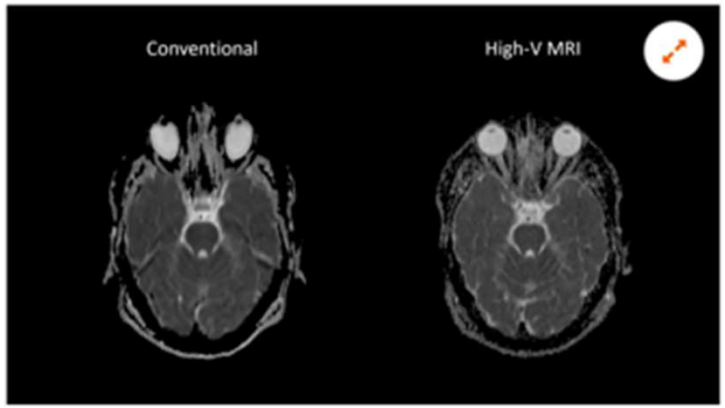

Reduced susceptibility challenges with High-V MRI

Susceptibility artifacts are a well know phenomena in MRI. One prominent example for such artifacts are at air-tissue interfaces, as they occur at the sinuses and orbits. The unique field strength of High-V MRI offers physical advantages that inherently reduce susceptibility artifacts. This leads to reduced geometric distortions in diffusion imaging which results in improved diagnostic quality.

Mini-resonador

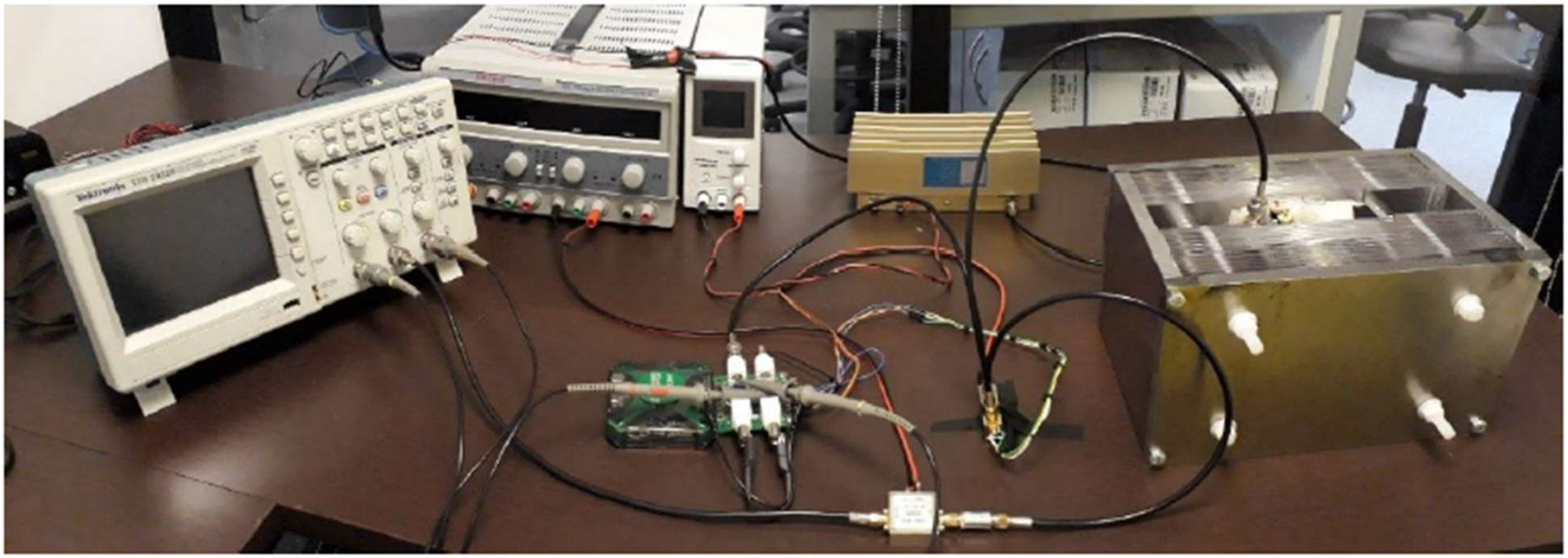

Figure 6: Tabletop in-house built 0.1T MRI scanner.

Susceptibility Tensor Imaging

$$\Delta f(\mathrm{k}) = \gamma B_o \left(\frac{1}{3} \hat{\mathbf{H}}^T \chi(\mathrm{k}) \hat{\mathbf{H}} - \hat{\mathbf{H}} \cdot \mathrm{k} \frac{\mathrm{k}^T \chi(\mathrm{k}) \hat{\mathbf{H}}}{k^2} \right)$$

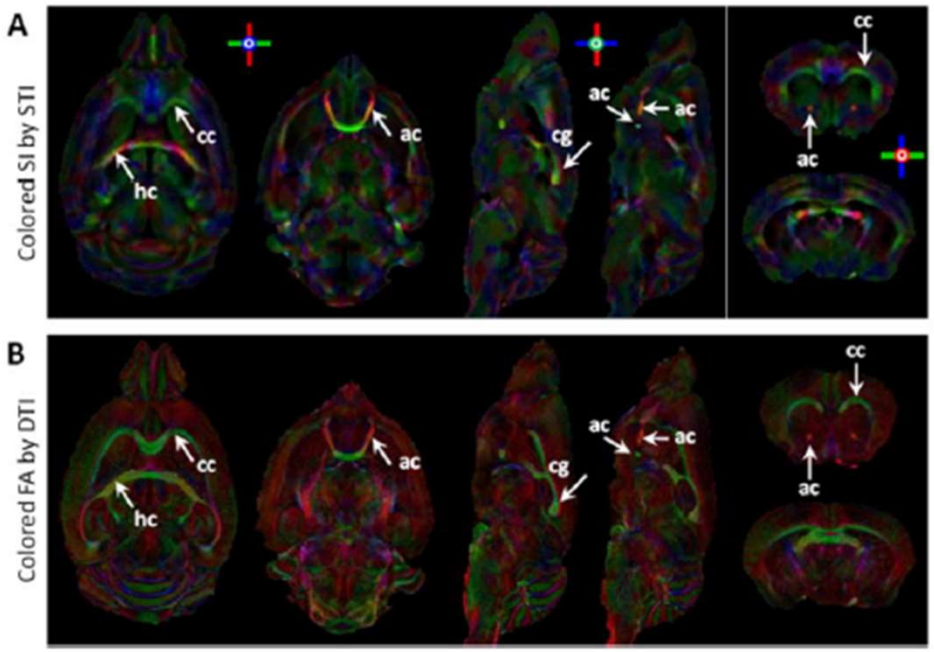

Figure 3: Susceptibility index from a STI acquisition showing the dependence of directions (A) and Fractional Anisotropy in a DTI acquisition (B) [?].

Otros proyectos (pasados)

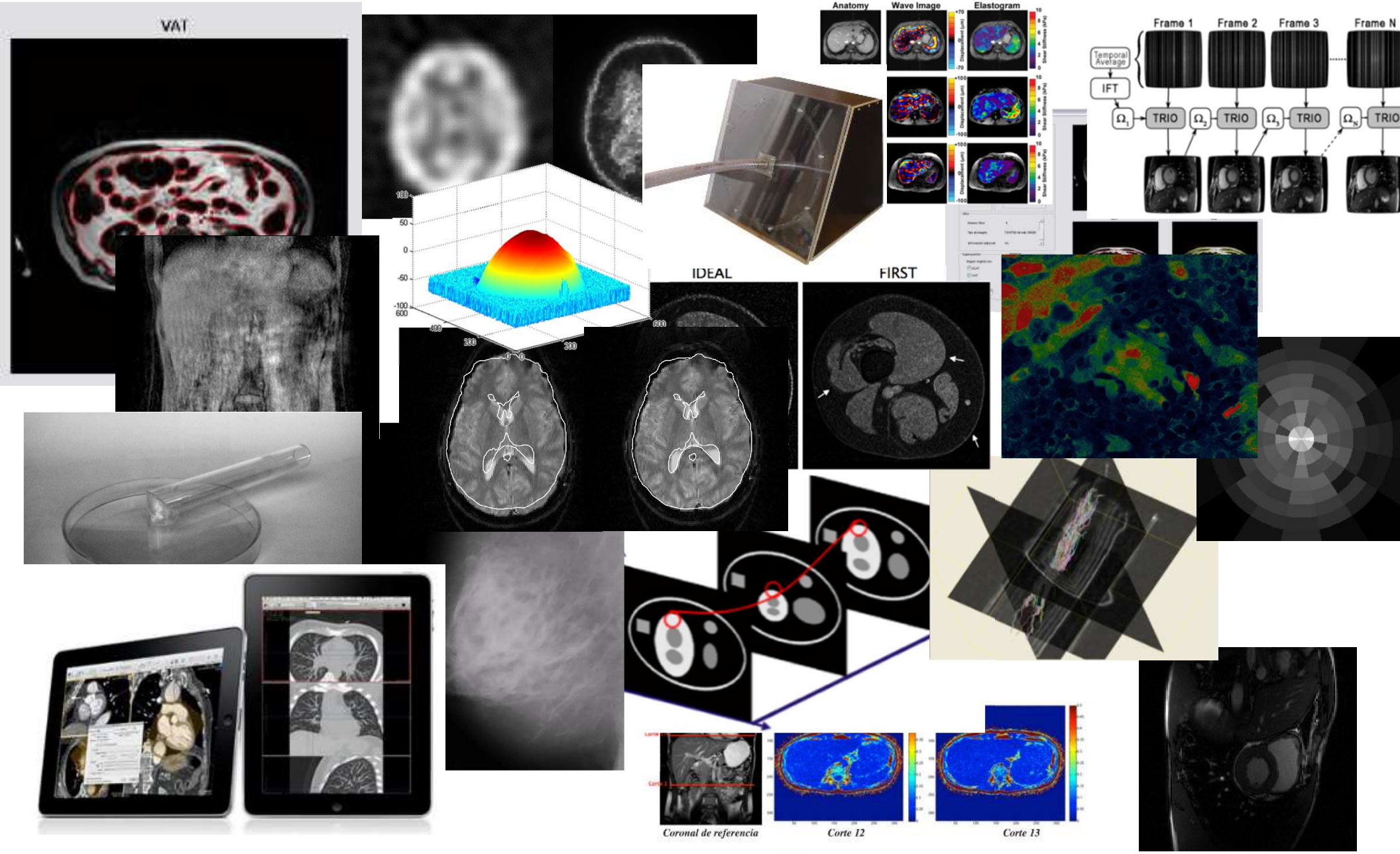

PONTIFICIA UNIVERSIDAD CATÓLICA DE CHILE

Biomedical Imaging Center

iibm Instituto de Ingeniería Biológica y Médica

Oportunidades de investigación

Pablo Irarrázaval
pim@uc.cl